

Is occlusion of the main pancreatic duct by thermal ablation really safe? A surgical innovation assessed according to IDEAL recommendations

Xavier Moll, Dolors Fondevila, Félix García-Arnas, Juan J. Pérez, Benedetto Ielpo, Patricia Sánchez-Velázquez, Luis Grande, Sofía Jaume, Aleksandar Radosevic, Luis Barranco, Enrique Berjano, Fernando Burdio & Anna Andaluz

To cite this article: Xavier Moll, Dolores Fondevila, Félix García-Arnas, Juan J. Pérez, Benedetto Ielpo, Patricia Sánchez-Velázquez, Luis Grande, Sofía Jaume, Aleksandar Radosevic, Luis Barranco, Enrique Berjano, Fernando Burdio & Anna Andaluz (2023) Is occlusion of the main pancreatic duct by thermal ablation really safe? A surgical innovation assessed according to IDEAL recommendations, *International Journal of Hyperthermia*, 40:1, 2203888, DOI: [10.1080/02656736.2023.2203888](https://doi.org/10.1080/02656736.2023.2203888)

To link to this article: <https://doi.org/10.1080/02656736.2023.2203888>



© 2023 The Author(s). Published with license by Taylor & Francis Group, LLC



Published online: 01 May 2023.



[Submit your article to this journal](#)



[View related articles](#)



[View Crossmark data](#)

Is occlusion of the main pancreatic duct by thermal ablation really safe? A surgical innovation assessed according to IDEAL recommendations

Xavier Moll^{a,b} , Dolors Fondevila^a , Félix García-Arnas^a , Juan J. Pérez^c , Benedetto Ielpo^d ,
Patricia Sánchez-Velázquez^d , Luis Grande^d , Sofía Jaume^d , Aleksandar Radosevic^e , Luis Barranco^f ,
Enrique Berjano^c , Fernando Burdio^d  and Anna Andaluz^a 

^aDepartament de Medicina i Cirurgia Animals, Facultat de Veterinària, Universitat Autònoma de Barcelona, Barcelona, Spain; ^bFundació Hospital Clínic Veterinari, Universitat Autònoma de Barcelona, Bellaterra, Spain; ^cBioMIT, Department of Electronic Engineering, Universitat Politècnica de València, Valencia, Spain; ^dDivision of Hepato-Biliary and Pancreatic Surgery, Department of Surgery, Hospital del Mar, Barcelona, Spain; Hospital del Mar Medical Research Institute (IMIM), Barcelona, Spain; ^eDivision of Hepato-Biliary and Pancreatic Radiology, Department of Radiology, Hospital del Mar, Barcelona, Spain; Hospital del Mar Medical Research Institute (IMIM), Barcelona, Spain; ^fDivision of Endoscopy, Department of Digestive diseases, Hospital del Mar, Barcelona, Spain; Hospital del Mar Medical Research Institute (IMIM), Barcelona, Spain

ABSTRACT

Introduction: Pre-clinical studies suggest that thermal ablation of the main pancreatic duct (TAMPD) is more recommendable than glue for reducing postoperative pancreatic fistula (POPF). Our aims were (1) to analyze the changes in the pancreas of patients after TAMPD and (2) to correlate the clinical findings with those obtained from a study on an animal model.

Materials and methods: A retrospective early feasibility study of a marketed device for a novel clinical application was carried out on a small number of subjects ($n=8$) in whom TAMPD was conducted to manage the pancreatic stump after a pancreatectoduodenectomy (PD). Morphological changes in the remaining pancreas were assessed by computed tomography for 365 days after TAMPD.

Results: All the patients showed either Grade A or B POPF, which generally resolved within the first 30 days. The duct's maximum diameter significantly increased after TAMPD from 1.5 ± 0.8 mm to 8.6 ± 2.9 mm after 7 days ($p=.025$) and was then reduced to 2.6 ± 0.8 mm after 365 days PO ($p<.0001$). The animal model suggests that TAMPD induces dilation of the duct lumen by enzymatic digestion of ablated tissue after a few days and complete exocrine atrophy after a few weeks.

Conclusions: TAMPD leads to long-term exocrine pancreatic atrophy by completely occluding the duct. However, the ductal dilatation that occurred soon after TAMPD could even favor POPF, which suggests that TAMPD should be conducted several weeks before PD, ideally by digestive endoscopy.

ARTICLE HISTORY

Received 13 February 2023

Revised 11 April 2023

Accepted 12 April 2023

KEYWORDS



Duct occlusion; pancreatic duct; postoperative pancreatic fistula; thermal ablation; IDEAL recommendations

1. Introduction

To date, many attempts to occlude the main pancreatic duct (MPD) have been reported [1] and it is well known that ligation or occlusion of the MPD leads to complete exocrine atrophy of the pancreas, with apparent preservation of the endocrine pancreas and without inducing any significant clinical signs of pancreatitis [1]. Clinical studies involving the intraductal injection of glue into the MPD have been performed in two scenarios: (1) as a method of abolishing pancreatic secretion and pain in chronic pancreatitis [2,3] and (2) as a method of managing the pancreatic stump after pancreatectoduodenectomy (PD) to avoid postoperative pancreatic fistula (POPF) [4–8]. However, this procedure never found much acceptance among clinicians because of the high risk of failure in the form of recanalization of the MPD

(first indication) or POPF (second indication), which can affect more than 50% of the patients [9,10]. In spite of this, occlusion of the MPD (usually by glue or sutures) remains an option for management of the pancreatic stump after PD in 'difficult circumstances' [10], and in fact, it is currently employed and recommended by some groups [5,6,11], particularly when the risk of pancreatic fistula is high [8].

Our pre-clinical experience suggested that the thermal ablation of the main pancreatic duct (TAMPD) by radiofrequency (RF) leads to necrosis of the epithelium and fibrosis, resulting in shrinkage and occlusion of the MPD after one month, being superior to glue in terms of reducing POPF [12,13]. These results encouraged us to conduct TAMPD in very selective high-risk clinical POPF scenarios, in which thermal ablation of the main pancreatic duct was conducted intraoperatively just before Blumgart-type pancreatic-jejunal

CONTACT Anna Andaluz  anna.andaluz@uab.cat  Departament de Medicina i Cirurgia Animals, Facultat de Veterinària, Universitat Autònoma de Barcelona, Barcelona, Spain

© 2023 The Author(s). Published with license by Taylor & Francis Group, LLC

This is an Open Access article distributed under the terms of the Creative Commons Attribution License (<http://creativecommons.org/licenses/by/4.0/>), which permits unrestricted use, distribution, and reproduction in any medium, provided the original work is properly cited. The terms on which this article has been published allow the posting of the Accepted Manuscript in a repository by the author(s) or with their consent.

anastomosis [14]. After analyzing the course of the first eight first patients, we unfortunately noted that TAMPD did not completely avoid POPF. Since we know little about pancreatic tissue changes after TAMPD in the first weeks (as all our pre-clinical experience was based on one-month survival), we planned a multidisciplinary study to analyze TAMPD-induced changes in the early days, the period in which the risk of POPF is deemed to be particularly challenging. We here analyze the clinical data and the results of an experimental study. Both methods contribute to improve the new technique according to IDEAL recommendations, which emphasize that surgical innovation is frequently non-linear and require iterative phases in the animal setting [15].

The manuscript is organized as follows: first, the device used for ductal occlusion is technically described, as well as the materials and methods used in the preliminary clinical study, computer modeling and preclinical experiments based on an animal model. The Results section begins by describing the findings of the preliminary clinical study, continues with the results of the computational model and ends with the preclinical results in the animal model. Finally, in the Discussion section, the results are analyzed as a whole, presenting a theory that allows explaining the clinical findings in light of the computational and preclinical results.

2. Material and methods

2.1. Thermal ablation device

TAMPD was conducted by the off-label use of the 3-cm-long ClosureFast[®] system (Medtronic, Mansfield, MA, USA), originally designed to treat varicose veins through thermal endovenous occlusion [16]. The ClosureFast[®] applicator consists of a 7 Fr catheter with a coil on its surface which is heated by the passage of RF current through the coil itself [17] (see Figure 1(A–D)), which means that no electrical RF current flows into the tissue and heat is applied only to the tissue surrounding the device, so that the term ‘radiofrequency ablation’ applied to the ClosureFast[®] system is a bit confusing. The energy protocol is simple and established directly by the manufacturer and consists of 20 s applications with temperature control at 120 °C (the system takes about 4 s to reach this target value).

2.2. Initial clinical experience

2.2.1. Study protocol and inclusion criteria

This retrospective study was approved by the Clinical Research and Ethics Committee of our institution (Ref. 2020/9514/I). All patients gave their written informed consent, including giving permission to publish results, keeping

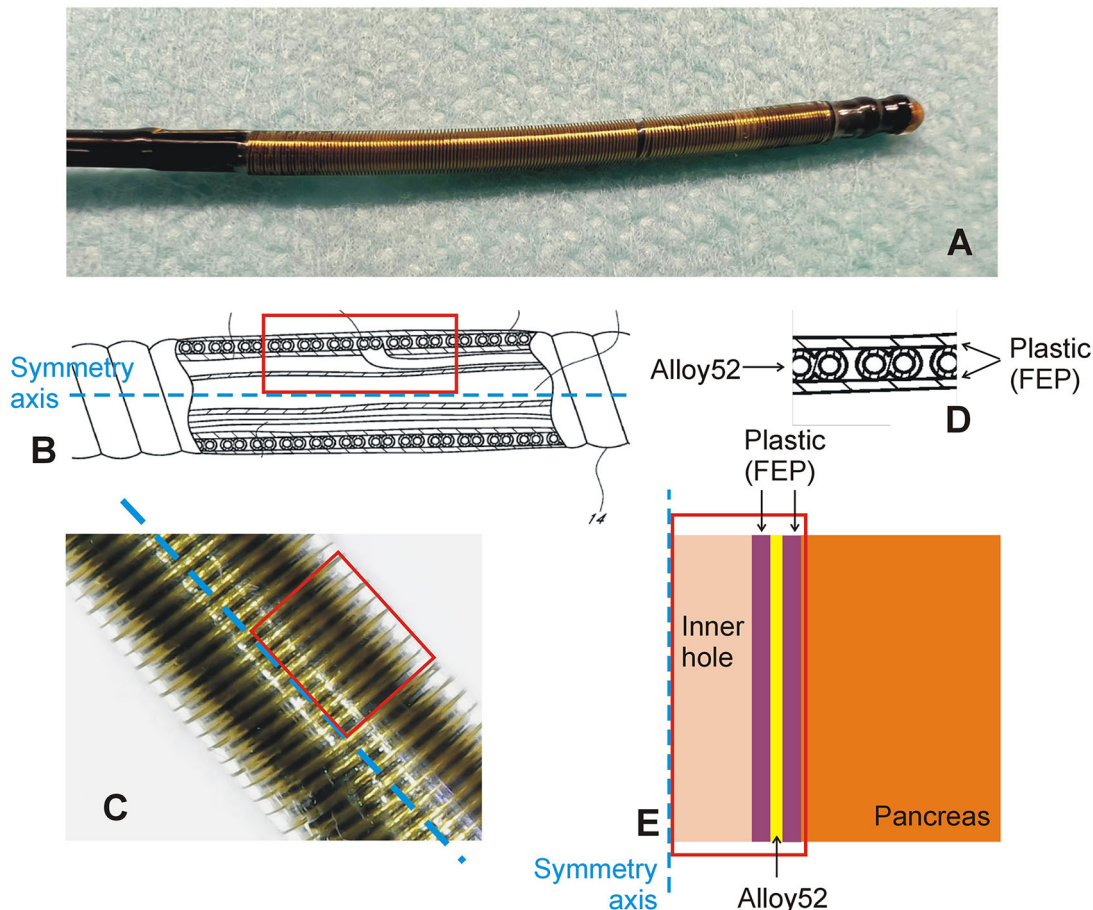


Figure 1. Thermal ablation applicator. (A): Thermal ablation device. (B) Technical drawing of the catheter for endoluminal thermal ablation model ClosureFast[®] (Medtronic, Mansfield, MA, USA) showing the inner elements and layers. The blue dashed line represents the catheter axis. (C) Detail of the catheter surface showing the helical structure of conductors through which the electric current circulates. (D) Detail of the concentric layers of Teflon and Alloy on which the geometry of the computational model was based (E).

strictly to maintaining patient confidentiality. The study was conducted in accordance with principles of the Declaration of Helsinki and Good Clinical Practice guidelines. We retrospectively analyzed eight patients who had undergone TAMPD in the context of an early feasibility study, i.e. a limited clinical investigation of a marketed device for a novel clinical application to evaluate the initial clinical safety in a small number of subjects (<10) [18].

TAMPD was conducted as described in [14] to manage the pancreatic stump after pancreatoduodenectomy (PD) with a high risk of POPF (CALLERY over 7) [19] immediately after performing Blumgart-type pancreaticoyeyunal anastomosis (BPA) in seven cases and in the context of a repair because of POPF seven days after previous PD, with BPA reconstruction in one case. The period of time included was from July 2020 to October 2021, in which all the patients suitable for PD were assessed for eligibility after being discussed by the multidisciplinary tumor board for pancreatic disorders. The inclusion criteria were as follows: age 18 years or older and a high risk of pancreatic fistula (CALLERY over 7) after PD for any reason. Exclusion criteria were: American Anesthesia Association (ASA) Classification >III or refusal to participate in the study.

2.2.2. Postoperative care and follow-up

The postoperative care of the treated patients followed the standards of care for patients undergoing PD in our institution, recording any clinically relevant intra- and post-operative (PO) outcome indicators associated with surgical performance as the severity of complications graded by the Clavien-Dindo Classification [20]. POPF was graded by the classification of the updated International Study Group on Pancreatic Fistula [21].

2.2.3. Morphological analysis

As in [22], morphological changes of the remaining pancreatic pancreas were assessed by computed tomography (CT) images at 7, 15, 30, 60 and 365 PO days using two parameters: (1) the transverse diameter of the pancreas measured perpendicular to the axis of the pancreas at 2 cm from the pancreatic tail and (2) the maximum MPD diameter. Five-millimeter consecutive sections were analyzed through the abdominal dual phase (portal and equilibrium) helical CT.

2.3. Computer modeling

A computational model was built to simulate the heat conducted through pancreatic tissue by an ablation catheter similar to the one used in the clinical and pre-clinical studies. The model solved the Bioheat Equation by ANSYS (ANSYS,

Canonsburg, PA, USA). Figure 1(E) shows the geometry of the computational model, which consists of a fragment of pancreas and MPD. The thermal ablation device was assumed to be in firm contact inside the MPD. The spatial arrangement of tissue, MPD and applicator involved an axis symmetry, which allowed us to consider a two-dimensional model. The applicator was 7Fr in diameter and 30 mm long and was internally simplified as a structure of concentric layers based on the information included in the device's patent [17]: an empty area in the interior (1.49 mm diameter), surrounded by two nonstick plastic layers of FEP (fluorinated ethylene propylene, 0.15 mm each), with an interior Alloy52 layer (0.12 mm thick) that simulates the resistive conductors through which the electric current circulates to induce heating.

The governing equation was the Bioheat Equation, in which the metabolic heat term was ignored since it was negligible in comparison to the other terms (11.89 W/kg heat generation rate, which is equivalent to $\sim 13 \text{ mW/mm}^3$ by using a 1087 kg/m^3 density [23]). The blood perfusion term Q_p computed was set to zero at those points at which a temperature of 50°C was reached, which allowed modeling the loss of blood perfusion due to the thermal destruction of the tissue. In order to model the vaporization in the tissue after reaching 100°C , the Bioheat Equation was modified as a balance of enthalpy changes as described in [24], considering the water mass fraction in the pancreas as 73.08% [25].

The thermal properties of the model elements are shown in Table 1 (pancreas characteristics were obtained from [23], and the catheter materials from [www.matweb.com, accessed 13 February 2023]). Maximum, average and minimum values were considered for the pancreas characteristics. The three values of perfusion rate for the pancreas (0.009 , 0.014 and 0.030 s^{-1}) were the minimum, average and maximum perfusion rates reported in [23], i.e. 469, 767 and 1640 ml/min/kg (data from 13 studies). The initial temperature in the entire model was 37°C . A null thermal flux was used on the symmetry axis and a constant temperature of 37°C was fixed on the outer surfaces of the model (this was also the initial temperature value). Thermal excitation was modeled by setting the temperature value in the alloy zone using a ramp from 37 to 120°C during the first 5 s, followed by a plateau to complete 20 s of treatment. After this, the condition was eliminated by releasing the temperature of this subdomain. This zone corresponds to the zone in which the inner temperature sensor is situated to control the heating process.

The ablation zone size was computed by the 55°C isotherm contour and the Arrhenius thermal damage index Ω . The parameter values of this index are those of each tissue type and process analyzed. Due to the lack of experimental data for heat-induced necrosis of the pancreas, we used the values $A = 7.39 \times 10^{39} \text{ s}^{-1}$ and $E_a = 2.577 \times 10^5 \text{ J/mol}$, broadly

Table 1. Physical characteristics of tissues and materials of each element used in the model.

Element/material	k (W/m-K)	ρ (kg/m ³)	c (J/kg-K)
Plastic / FEP	0.22	2120	1200
Resistive coil / alloy52	14	8300	481
Pancreas minimum, average, maximum, (number of studies)	0.47, 0.51, 0.59 ($n = 5$)	1045, 1087, 1128 ($n = 2$)	2822, 3164, 3506 ($n = 2$)

Note: k : thermal conductivity; ρ : density; c : specific heat.

used in radiofrequency ablation computer studies [24]. Lesion size was calculated by considering all the points of the tissue at which $\Omega \geq 1$, which is equivalent to a 63% cell death probability.

The model was verified in terms of outer dimensions and meshing. The outer dimensions of the fragment of pancreas were estimated by means of a convergence test to avoid boundary effects. In this test, the temperature reached at several points away (1–5 mm) from the center of the applicator was used as the control parameter. We first considered a tentative spatial (i.e. minimum meshing size) and temporal resolution. To determine the appropriate parameters we increased their values by equal amounts. When the difference in the temperatures reached at those points between consecutive simulations was less than 0.5%, we considered the former values to be adequate. We then determined adequate spatial resolution by means of a similar convergence test using the same control parameters as in the previous test. Discretization was spatially heterogeneous: the finest zone was always at the applicator-tissue interface, where the largest thermal gradient was produced. In the tissue, grid size was increased gradually with distance from the applicator-tissue interface. The model had 20,460 nodes and 9,200 triangular elements. The convergence tests provided the following parameters: a distance of 4 cm from any point of the catheter until the outer limit of the model, minimum and maximum mesh size of 0.25 and 3 mm, respectively, and a time step ranging from 20 to 50 ms.

2.4. In vivo study on animals

2.4.1. Animal model, experimental groups and surgical procedure

Fifteen female Landrace pigs (85.1 ± 8.8 kg weight) were used in this study. The animal research protocol followed the guidelines approved by the Ethical Commission of the Universitat Autònoma de Barcelona (Authorization Number CEEAH 3487 and DMAH 9583) and the Government of Catalonia's Animal Care Committee. Three groups were established according to the postoperative follow up: 0-day ($n=3$), 7-day ($n=6$) and 30-day ($n=6$). All the surgical procedures were performed by the same surgical team (AA and XM), *via* open laparotomy and enterotomy. After locating the pancreatic papilla, the ablation catheter was gently advanced as far as possible into the MPD (see Figure 2). After conducting thermal ablation, the enterotomy and laparotomy were closed in the conventional manner. The animals in the 0-day Group were sacrificed immediately after ablation, while those in the 7- and 30-day Groups were kept alive for 7 and 30 days.

2.4.2. Preoperative care and anesthesia in the animal model

Preoperative care and anesthesia were provided by fully trained veterinary staff. All the animals were fasted for 12 h before surgery. After initial sedation with a combination of azaperone (4 mg/kg), ketamine (10 mg/kg) and midazolam

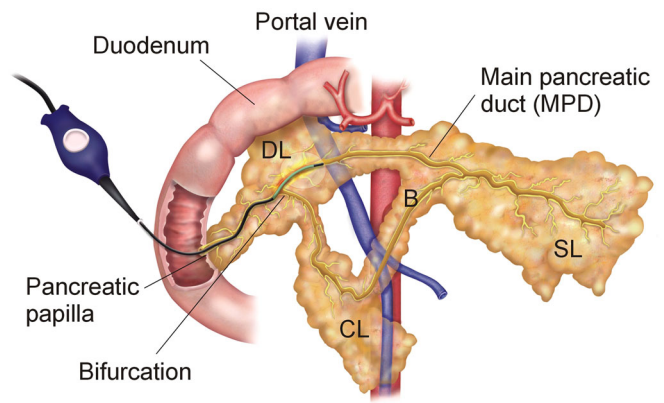


Figure 2. Animal model. Endoluminal thermal ablation of the main pancreatic duct (MPD) conducted using the ClosureFast[®] system (Medtronic, Mansfield, MA, USA). SL: splenic lobe; DL: duodenal lobe; CL: connecting lobe (CL); B: Bridge. Note that the connecting lobe and bridge are present in the pig anatomy but not in the human pancreas.

(0.2 mg/kg), intravenous access was obtained through marginal ear-vein cannulation. Analgesia was given previous to general anesthesia (morphine 0.2 mg/kg IV). The anesthetic induction phase was performed with propofol (4 mg/kg IV). The trachea was intubated, and anesthesia maintained with 2–2.5% isoflurane IsoVet (B. Braun VetCare Spain, Rubí, Spain) in 100% oxygen through a semi-closed circular anesthetic system. Ventilation was controlled using intermittent positive pressure ventilator (Dräger Fabius plus, Lübeck, Germany) to maintain normocapnia during the entirely anesthetic period. An infusion of lactated Ringer's solution at a rate of 10 ml/kg/h was administered during the perioperative period *via* the auricular vein. Throughout the surgical process, temperature, cardiac frequency, respiratory frequency, capnography, arterial pressure, pulse and electrocardiography were monitored using a patient multifunction monitor (Dräger Vista 120, Lübeck, Germany).

2.4.3. Postoperative care and necropsy in the animal model

Animals in the 7 and 30-day Groups received water *ad libitum* for the first 24 h and subsequently were fed appropriate food twice daily. A delayed-acting antibiotic (ceftiofur 5 mg/kg IM) was administered (animals with postoperative follow-up) at the end of the surgery procedure. All the animals were inspected twice a day for the first seven postoperative days to detect any clinical signs of pancreatic leak or sepsis and to monitor debit and state of abdominal drains. They received morphine (0.2 mg/kg IM, q8h) for the first 16 postoperative hours and meloxicam (0.2 mg/kg IM, q24 h) for postoperative analgesia in the first five postoperative days. They were also given a 100 µg/h fentanyl patch for four days after the surgical procedure. Peripheral blood was collected for measurement of serum amylase levels prior to the surgical procedure for all Groups, on days 2 and 7 PO for 7-day and 30-day Groups, and four weeks before euthanasia for 30-day Group. The blood samples were centrifuged at 2500 × G for 10 min to extract the serum. Biochemical laboratory parameters were determined at the Centralized Analysis Center of the Universidad Autònoma de Barcelona,

Veterinary Faculty, by technicians who were unaware of the study groups.

The primary outcome was to determine the histological changes in the tissue after endoductal thermal ablation. Secondary outcomes were intraoperative complications, alterations in stool consistency, extravasation of the iodinated contrast during necropsy and other postoperative clinical parameters (anorexia, emesis, lethargy and narcotic need). For necropsy, the animals were sedated with an IM combination of azaperone (4 mg/kg), ketamine (10 mg/kg) and midazolam (0.2 mg/kg) and then euthanized with an overdose of sodium pentobarbital (200 mg/kg IV). Prior to completing the necropsy, an exploratory laparotomy was performed and the peritoneal cavity was assessed for excessive adhesions, free peritoneal fluid or any undrained collection/abscess.

2.4.4. Duct permeability test and histopathological analysis

During necropsy, the pancreas (stump, uncinate process and head) was dissected and removed. The MPD of each removed pancreas duct was then identified and cannulated with an angiocatheter through both the ampulla of the duodenum and the pancreas tail (once cut). Duct permeability was evaluated by injecting 1–2 ml of iodinated contrast Xenetix 300 mg/mL (Guebert Laboratories, Princeton, NJ, USA) in an antegrade and retrograde manner (i.e. from the papilla and from the tail, respectively). After a contrast injection, radiological images were obtained using a fluoroscope OEC Fluorostar (General Electric Healthcare, Chicago, IL, USA). The specimens were histologically analyzed by light microscope.

The specimen was immersed in 10% buffered neutral formalin for further histopathology processing. Three-mm thick consecutive sections of the entire pancreas were taken from each specimen. Two to four samples of the splenic lobe and connecting duodenal lobe were routinely processed and paraffin-embedded, cut to a thickness of 5 μ m, stained with hematoxylin and eosin (H&E) and evaluated by light microscope.

2.5. Statistics

Data were analyzed using SPSS version 19.0 (IBM, Armonk, NY, USA). Normality was tested by the Shapiro-Wilk test. Continuous data of repeated measurements of the data obtained from the initial clinical experience were evaluated by Wilcoxon's nonparametric test. Non-linear fits (i.e. higher-order regression models) and linear regression models were also performed to determine the best fit equations for morphological measurements. The best goodness of fit of the models was individually assessed both graphically and by R^2 for each group, which can be interpreted as the proportion of the total variability explained by the model. The Wilcoxon test was used to evaluate amylase levels between the time periods of the data obtained from the animal study. A p value $<.05$ was considered to be significant.

3. Results

3.1. Preliminary clinical experience

3.1.1. Clinical outcomes of the patients

In all cases the diameter of the MPD before ablation was under 3 mm (mean value 1.5 ± 0.8 mm) and the pancreas was deemed as 'soft' in all cases, demonstrated to be at highest risk of POPF after PD. The TAMPD protocol in terms of energy deposition was completed in all cases as previously described, both in the elective cases and after a reoperation, because of POPF-associated life-threatening bleeding. In the second case, the pancreas anastomosis was disconnected from the bowel and the remaining pancreas left in place after the TAMPD procedure and coagulation of the transection line with a radiofrequency-assisted device. Four patients were operated on the diagnosis of pancreas adenocarcinoma, one on periampullary carcinoma, one on GIST tumor, one on neuroendocrine tumor and one on IPMN tumor. The length of stay was 24.6 ± 10.8 days, with a mean follow-up of 555 days (361–771 days). As the single mortality after the TAMPD procedure was at 543 days because of a non-procedure related liver metastasis, no surgical mortality (90-days PO) was caused by the procedure.

Overall, all the patients were diagnosed with POPF: 3 with Grade A – not clinically relevant– (37.5%), 5 with Grade B (62.5%) and 0 with Grade C (0%). Six out of 8 POPD (75%) resolved before 30 days PO. In all cases, there was a slight increase of serum lipase immediately after TAMPD, with a subsequent rapid return to normal (see Figure 3). No clinically relevant signs of pancreatitis were observed in any case. During the clinical follow-up, only one new onset of diabetes mellitus was observed (one of eight cases) and seven of eight patients (87.5%) needed pancreatic enzyme supplements.

3.1.2. Morphological analysis

Figure 4 shows CT images of the changes in the pancreas after TAMPD. The transverse diameter of the remaining pancreas significantly increased from 1.84 ± 0.38 cm to 2.81 ± 0.76 cm on day-7 PO ($p = .012$) and then gradually reduced to 1.49 ± 0.63 cm at 365 days PO (linear fit, $R^2 = 0.16$, $p = .01$), which was less than before TAMPD, but without reaching statistical significance ($p = .058$) (Figure 5(A,B)).

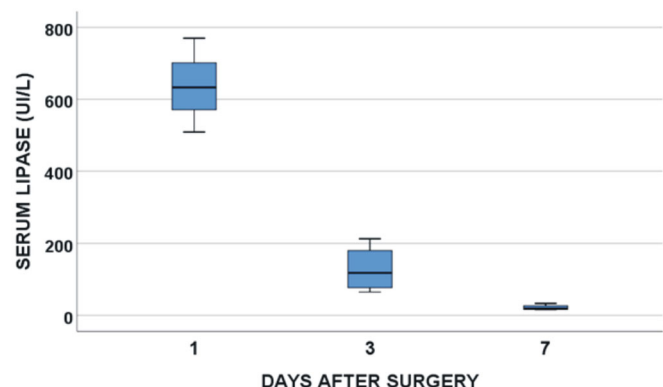


Figure 3. Clinical results. Serum lipase concentration throughout the postoperative period in patients after TAMPD. Note that the slight increase of first day is followed by a rapid decrease afterward.

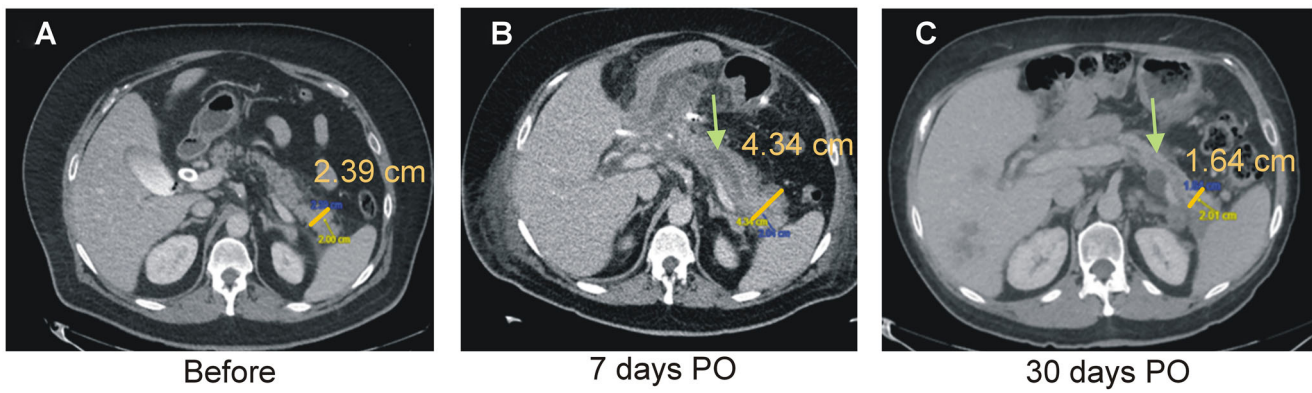


Figure 4. Clinical results. Typical CT images before (A), 7 days (B) and 30 days after TAMPD (C). Both the transverse diameter of the remaining pancreas (clear bar) and maximum diameter of the MPD (green arrow) increased at 7-day PO and then reduced at 30-day PO.

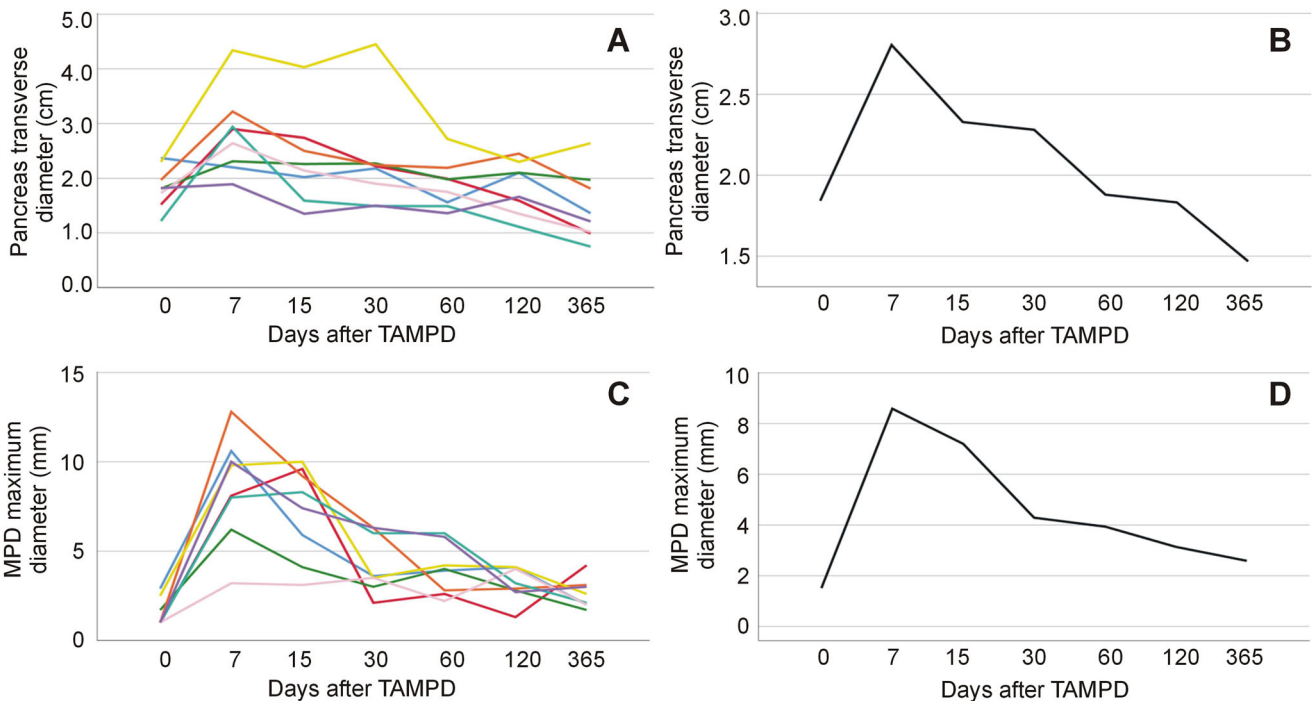


Figure 5. Clinical results. Post-operative progress of the transverse diameter of the remnant pancreas thickness (A,B) and maximum diameter of the main pancreatic duct (MPD) (C,D) in eight patients treated with thermal ablation of the MPD. Each patient is represented by a single-color line in left panels, while mean values (optimized scale) are shown in right panels. Note that the steep increase of pancreas diameter within the first week is followed by more slow decrease afterward. Interestingly, the final measurements of the pancreas diameter are below the initial values in all cases, which is consistent with pancreas atrophy of the stump. A similar behavior was observed in the MPD maximum diameter.

The maximum diameter of the MPD also significantly increased from 1.5 ± 0.8 mm to 8.6 ± 2.9 mm at 7 days ($p = .025$) and then reduced non-linearly to 2.6 ± 0.8 mm at 365 days PO, with the best fit following an inverse curve ($R^2 = 0.51$; $p < .0001$) (Figure 5(C,D)). The apparently thickened MPD in the CT at 7 days PO was rapidly reduced in the following three weeks.

3.2. Computer results

The computer results are shown in Figure 6. They predicted a depth of the ablated zone around the duct at 20 s of 1.85 ± 0.06 mm using the Arrhenius model and of 1.64 ± 0.06 mm using the 55°C isotherm.

Note that although we set a temperature of 120°C in the alloy zone, the computer simulations showed temperatures much lower on the ablation catheter ($\sim 97^\circ\text{C}$) and 1 mm away ($\sim 66^\circ\text{C}$). In order to confirm this huge thermal gradient experimentally, we conducted a complementary bench test by placing a micro-thermocouple IT-21 (Physitemp Instruments, Clifton, NJ, USA) on the catheter surface completely surrounded by a porous plastic material submerged in a bath at 37°C . This thermocouple was totally sheathed in Teflon and had a diameter of 0.4 mm and 80 ms time constant. During each heating cycle, we observed that the maximum temperature at the sensor gradually increased to $\sim 80^\circ\text{C}$ at 10 s, which confirms that the tissue applied to the tissue is always lower than 120°C , since this value only

corresponds to the one measured by the sensor inside the catheter.

3.3. In vivo experimental results

3.3.1. Intraoperative performance and postoperative follow-up

There were no intraoperative deaths or major complications during surgery. One animal in the 7-day Group was excluded because of a bacterial contamination with purulent content

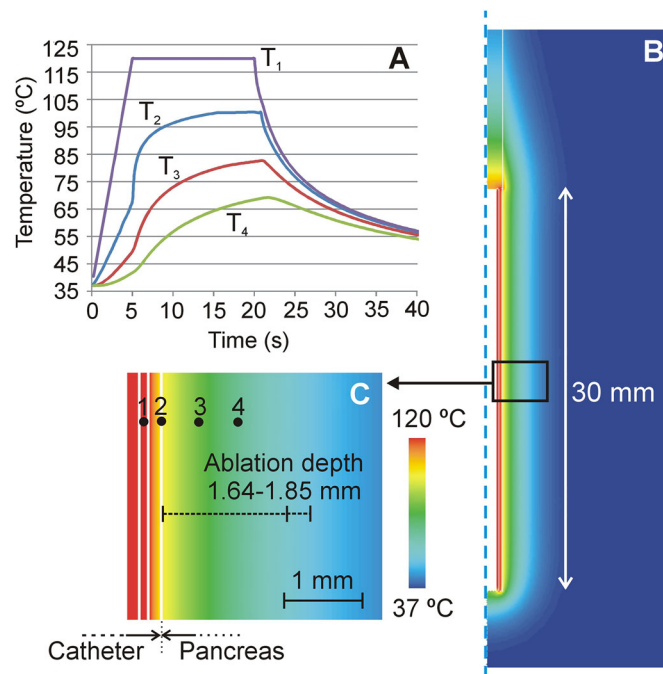


Figure 6. Computer results. (A) Temperature progress at several points of the model (1: inner conductors; 2: surface of the catheter; 3: at 0.45 mm from the surface; 4: at 1 mm from the surface). (B) Temperature distributions at 20 s in the catheter and pancreas. (C) Detail of the temperature in the proximity of the catheter, showing the position of the points where the temperature is plotted in Panel (A).

of the entire pancreas during necropsy, leaving five animals in the 7-day Group. Table 2 shows the post-operative outcomes. No animals died or suffered serious alterations during the postoperative period, with no alteration in stool consistency in any of the animals. In the 7- and 30-day Groups, serum amylase levels presented statistical differences ($p < .05$) on days 2 and 7 PO with preoperative and 30 days PO.

3.3.2. Macroscopic findings at necropsy and duct patency under fluoroscopic images

No macroscopic alteration was observed during the necropsy in animals in the 0-day Group. Fluoroscopic images showed MPD patency in all the animals, while an area of leakage of the iodinated contrast was seen in the thermal ablation zone in all the animals (Figure 7(A)). The results of the 7-day Group were not as homogeneous as those in the 0-day Group. Animals 7d-1, 7d-3, 7d-5 and 7d-6 showed an intrapancreatic dilatation with fluid content in the ablation zone and high levels of amylase. Fluoroscopic images showed MPD patency in animals 7d-1, 7d-2 and 7d-3, in which the thermal ablation zone could be detected by contrast leakage (Figure 7(B)). Conversely, animals 7d-5 and 7d-6 showed a totally obstructed MPD since the contrast was directed toward the connecting lobe (Figure 7(C)). As in the rest of the animals of the 7-day Group, the thermal ablation zone was identified by the presence of contrast leakage. Retrograde injection of contrast in these two animals confirmed the disruption of MPD permeability near the extravasation zone (Figure 7(D)).

No remarkable alterations were found during the necropsy of the 30-day Group, with complete occlusion of the MPD (without contrast leak) in all the animals. The extension of the thermal ablation zone could be easily identified in each case by retrograde injection of contrast from the pancreas tail. For instance, in animals 30d-1, 30d-2 and 30d-5, the proximal limit of the ablation zone was found before the

Table 2. Study variables before and after thermal ablation of main pancreatic duct.

Group	Animal	Plasma amylase levels (U/L)				Intrapancreatic fluid	Duct patency
		Preoperative	2 days PO	7 days PO	30 days PO		
0-day	0d-1	2791	–	–	–	–	Yes
	0d-2	2069	–	–	–	–	Yes
	0d-3	2718	–	–	–	–	Yes
	Median ± range	2718 ± 722	–	–	–	–	–
7-day	7d-1	2726	27,278	9828	–	23,980	Yes
	7d-2	2278	18,560	3404	–	Not found	Yes
	7d-3	2491	17,308	5034	–	499,890	Yes
	7d-4	2332	34,504	10,872	–	Discharged	–
	7d-5	2603	11,224	8483	–	192,640	No
	7d-6	3605	18,220	3958	–	192,640	No
	Median ± range	2547 ± 1327	18,390 ± 23,280 ^a	6758 ± 7468 ^{a,b}	–	–	–
30-day	30d-1	2763	8395	2771	2584	–	No
	30d-2	3543	42,811	38630	2814	–	No
	30d-3	3273	38,450	3118	3650	–	No
	30d-4	2635	19,380	2847	2602	–	No
	30d-5	2516	27,120	5577	2351	–	No
	30d-6	2071	47,788	29051	2172	–	No
	Median ± range	2699 ± 1472	32,785 ± 39,393 ^{a,c}	4347 ± 35,859 ^a	2593 ± 1478	–	–

^aSignificantly different from preoperative.

^bSignificantly different from 2 days PO.

^cSignificantly different from 30 days PO.

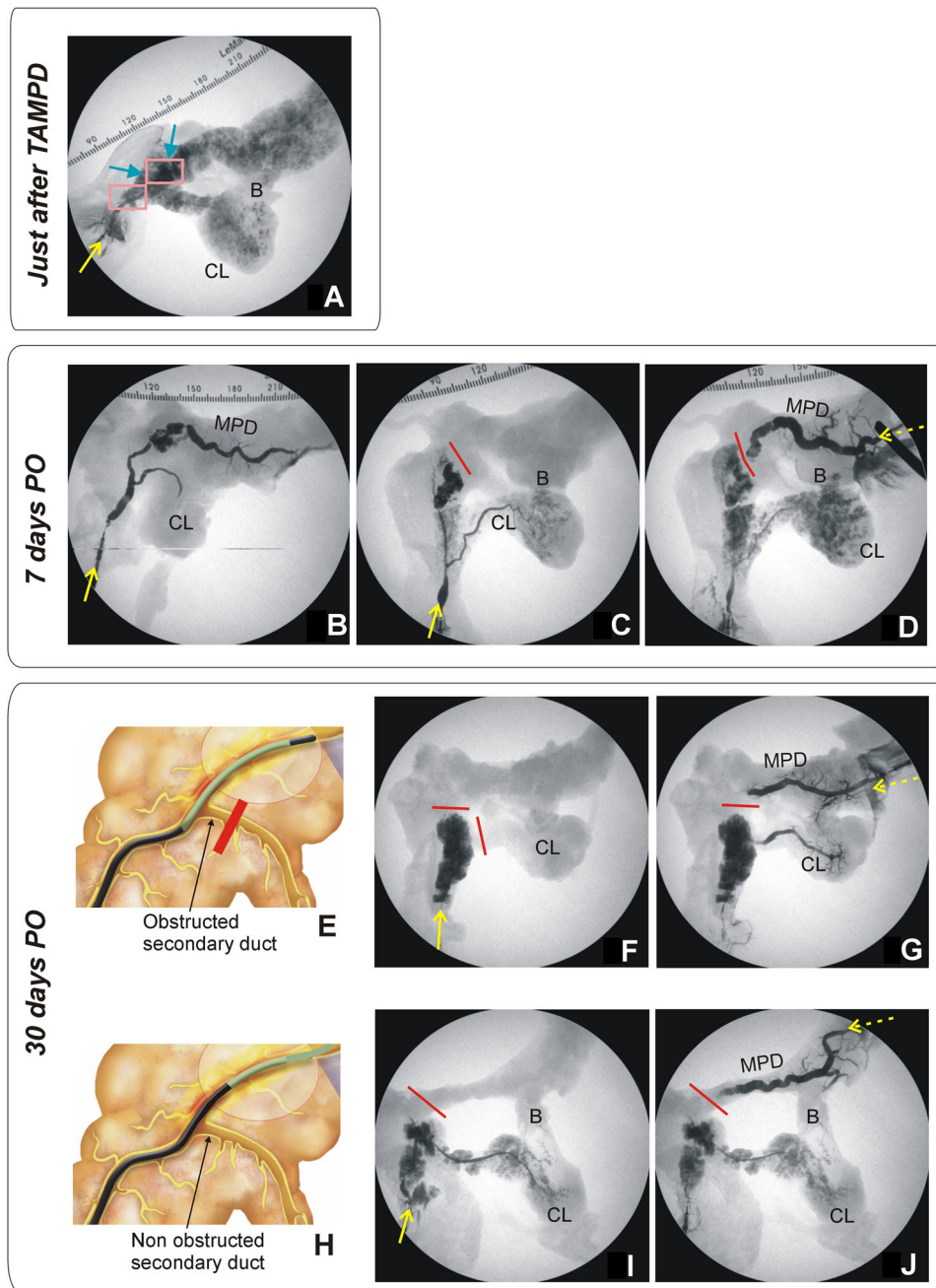


Figure 7. Animal model results. (A) Fluoroscopic image obtained during of the duct permeability test in 0-day Group. Iodinated contrast was injected through the MPD in anterograde, i.e. through papilla (yellow solid line), showing extravasation of the MPD in all cases (blue arrows), including the connecting lobe (CL). (B–D) Fluoroscopic images obtained in 7-day Group. While some animals showed MPD maintained patency when contrast was injected in an anterograde manner *via* the papilla (yellow solid line), i.e. the contrast occupied almost the entire length of the main duct and part of the connecting lobe (CL) (B), in other animals, the MPD was totally obstructed (red line) and the contrast was thus redirected toward the connecting lobe (C). In these animals, obstruction was confirmed when contrast was injected in a retrograde manner (yellow dashed line), i.e. from the most distal part of MPD (pancreas tail) (D). (F,G,I,J) Fluoroscopic images in 30-day Group. Although complete occlusion of the MPD was observed in all animals (red line represents the duct interruption), the injected contrast course revealed the relative position of the thermal ablation zone with respect to the bifurcation of the connecting lobe (secondary duct). (E–G) In some animals (e.g., 30d-5) anterograde (yellow solid line) and retrograde (yellow dashed line) injections of contrast suggested that the proximal limit of the thermal ablation zone was possibly before the bifurcation (as illustrated in (E)). (H–J) In other animals (e.g., 30d-4) anterograde and retrograde injections suggested that the proximal limit of the thermal ablation zone was possibly posterior to the bifurcation (as illustrated in (H)).

bifurcation with the connecting lobe (Figure 7(E)), preventing the contrast from flowing through the secondary duct of the uncinate portion in the cases of anterograde injection (Figure 7(F)) but not in those with retrograde injection (Figure 7(G)). In contrast, in animals 30d-3, 30d-4 and 30d-6, the proximal limit thermal ablation zone was possibly posterior to this bifurcation (Figure 7(H)), directing the contrast to

the uncinate portion during both the anterograde and retrograde injection (Figure 7(I,J)).

3.3.3. Histopathological findings

In 0-day Group, the pancreatic tissue around MPD showed a macroscopic whitish halo surrounded by an erythematous

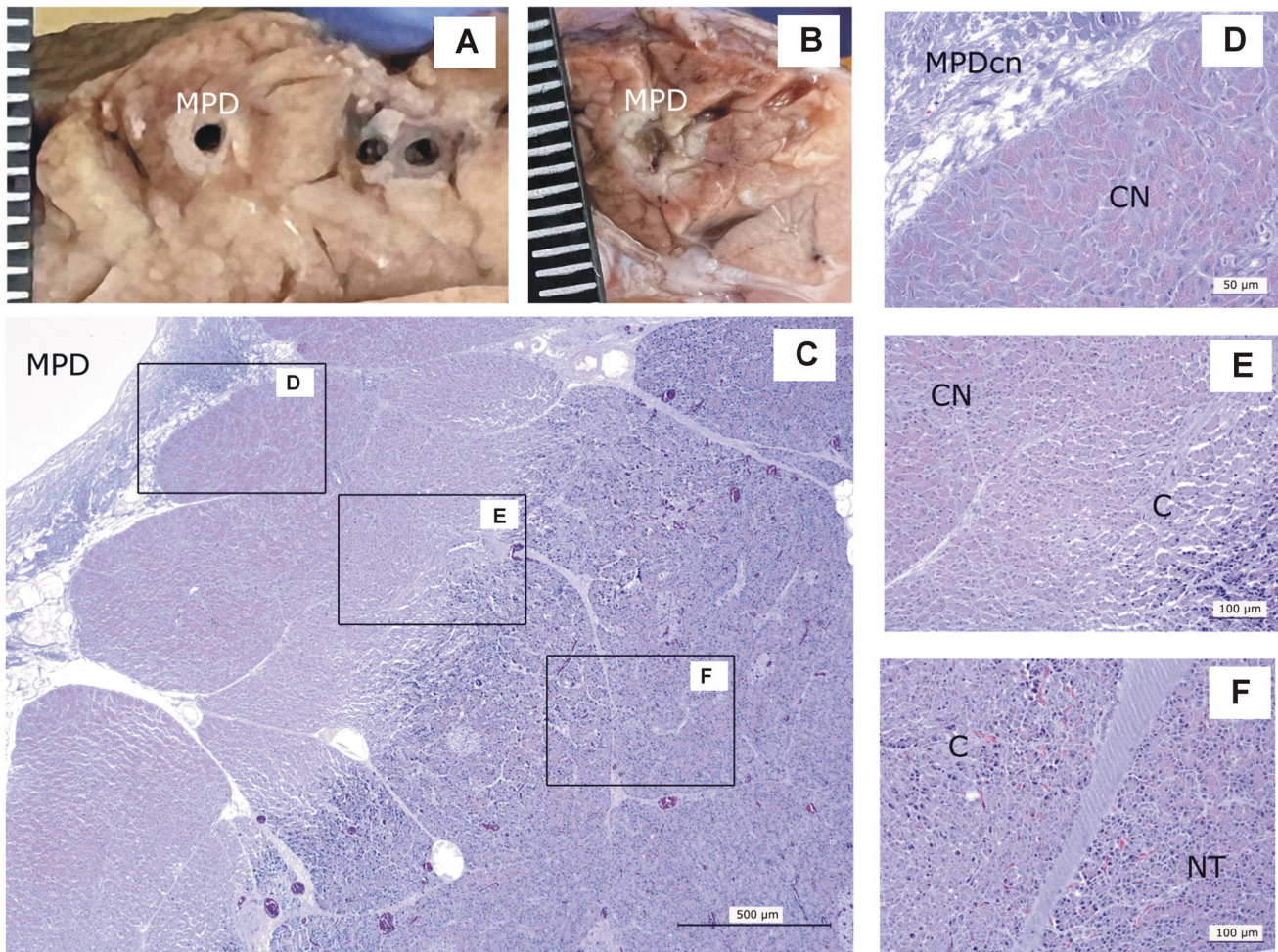


Figure 8. Animal model results. Histopathological findings of 0-day Group. (A,B) Macroscopic view of the main pancreatic duct (MPD) surrounded by a whitish and an erythematous halo. (C–F) Microscopic image (H&E): MPD with wall collagen necrosis (MPDcn) surrounded by three zones: Coagulation necrosis (CN) with intense zymogen granules eosinophilia (D), congestion (C) with disaggregated acini (E) and normal tissue (NT) (F). Scale in mm.

area (Figure 8(A,B)). Histologically, the duct had lost the epithelium and the wall collagen was necrotic (Figure 8(C–F)). Three zones were observed around the duct: coagulation necrosis with tissue preservation, a transitional zone of congestion with disaggregated acini and unaffected tissue. The necrotic depth around the duct was 1.5–2 mm in all cases, but the thickness of the congestion zone (erythematous halo) was highly variable between the animals, ranging from only 3 mm (Figure 8(A)) to 6 mm (Figure 8(B)).

In the 7-day Group, the ablated area was also clearly found macroscopically in all the animals, showing a 0.5–1 cm cavitory with irregular margins, content and colors, ranging from white to brown (Figure 9(A)). Microscopically (Figure 9(B–E)), there was a cavity with cellular debris, erythrocytes, fibrin and serous material surrounded by connective tissue with immature fibroblasts and collagen fibers, hemorrhages and scattered inflammatory infiltrate. The pancreatic tissue contained lobes with total or partial exocrine atrophy and others with no lesions. All the samples contained Langerhans islets.

All the animals in the 30-d Group presented a complete obstruction of the MPD at necropsy. During the histological analysis, dilation of the main and inter/intralobular pancreatic ducts was found in the pancreatic portion distal to the

obstruction in animals 30d-1, 30d-2 and 30d-5, as the ablation zone was created before the bifurcation of the main pancreatic duct and there was hence no communication with the uncinata portion (see Figures 7(E) and 10(D,E)). In animals 30d-3, 30d-4 and 30d-6, there was no macroscopic dilatation of the main pancreatic duct since in these animals the uncinata portion remained permeable. Histologically, the distal portion showed a complete homogeneous exocrine atrophy and Langerhans islets were preserved in all the animals (Figure 10(F)).

4. Discussion

One of the most troublesome and life-threatening complications of surgery such as POPF after PD is unlikely to be resolved completely and forever by a new surgical innovation at the first attempt, even if there are many previous experimental results on animals. Rather, as stated in the IDEAL statement issued in The Lancet by the Balliol Collaboration, innovation processes are naturally iterative, reverting to earlier stages (including computer modeling and studies on animal models) when substantial difficulties arise. Also, many technical modifications or refinements may be common during stage 2a ('development'), frequently with

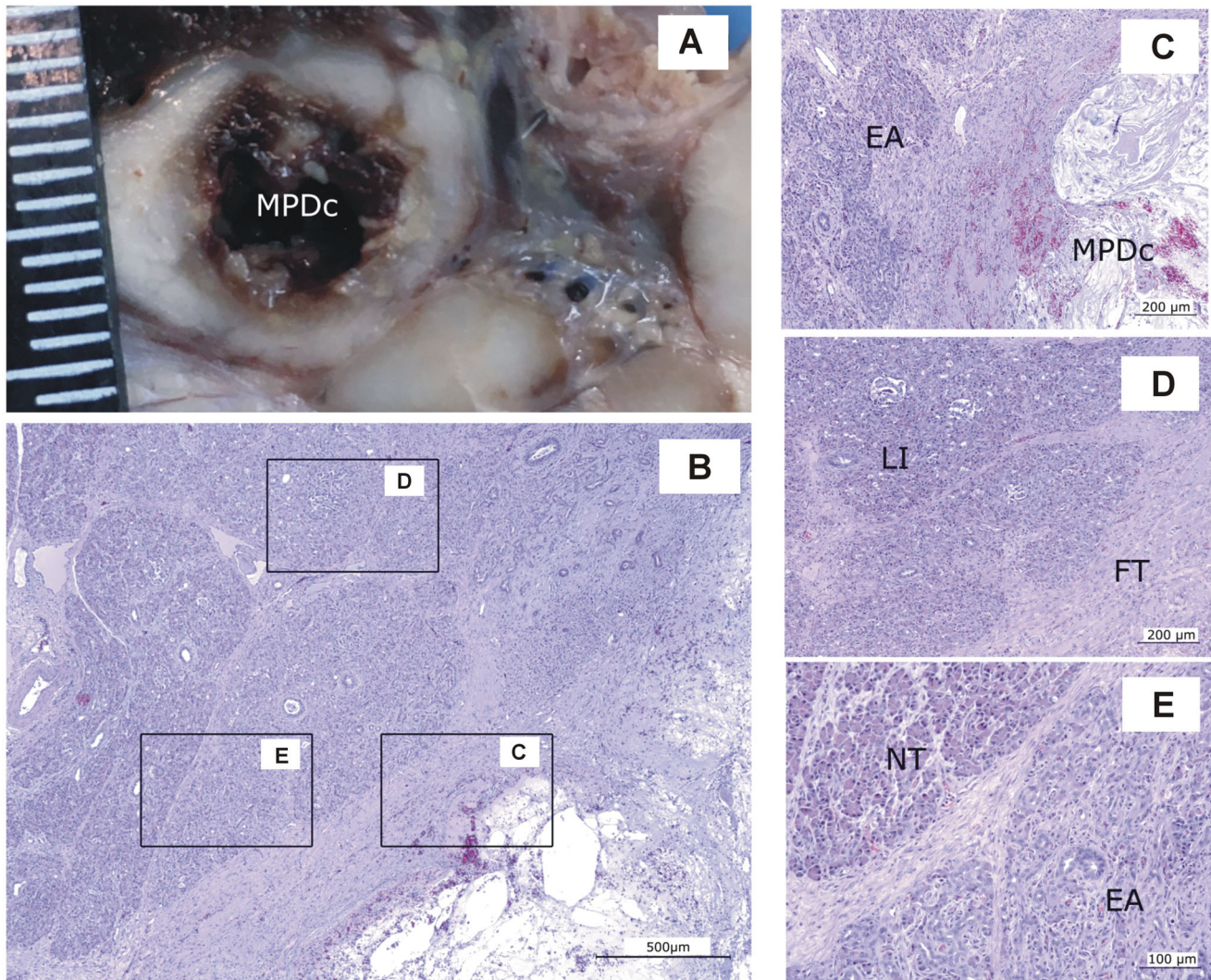


Figure 9. Animal model results. Histopathological findings of Group 7-day. (A) Macroscopic view of the main pancreatic duct (MPD) showing a large cavity (MPDc) with irregular brown margins. (B – E) Microscopic image (H&E). (C) Cavity with cellular debris and amorphous material (MPDc), complete exocrine atrophy (EA); (D) Fibrous tissue (FT) Langerhans islets preserved (LI). (E) Lobules with complete or partial exocrine atrophy (EA) and lobules without lesions (NT). Scale in mm.

less than ten treated patients [26]. This is precisely the position of TAMPD and where the real strength of the present study resides: TAPMD has been comprehensively evaluated by three different methods involving clinical surgeons, veterinary surgeons and biomedical engineers. After a preliminary intensive experience on the animals [12] we set out to test this technique in challenging clinical scenarios (first scenario: after PD Callery over 7 and second scenario: reintervention after PD because of POPD). In these challenging scenarios, the conventional treatment (pancreatic anastomosis) was deemed to lead to a high risk of clinically relevant POPD (B or C) of more than 67% [19] -first scenario- and particularly high mortality (>50%) in the second [27]. In our clinical experience, after reporting all the clinical cases performed to date (following the IDEAL reported guidelines) [15] no surgical mortality occurred in these challenging scenarios, although we found 62.5% of clinically relevant POPF in all cases. In spite of these relatively good or acceptable figures, the final clinical results were deemed suboptimal for a brand-new technique about which we know little in the first 30 days after ablation. Particularly, at this stage the following

doubts remained unsolved: (1) why did the thermal ablation of the MPD clearly seen in CT (see Figure 4(B)) almost disappear during the first two weeks? (see Figures 4(C) and 5(D)), (2) why did the thermal ablation not completely avoid POPF if the MPD was destroyed? and (3) why did POPF clearly resolve relatively soon (at 30 days of POPF) if it was present? The very early disappearance of the thermal ablation was completely different or even awkward in comparison to the conventional evolution of the necrotic tissue that leads to radiofrequency ablation of a pancreatic or liver tumor in which this encapsulated necrotic tissue is clearly seen even years after ablation [28,29]. The computer modeling and experimental studies provided valuable information on the early-stage thermal lesion characteristics and its later progress, suggesting a reasonable explanation of the above-mentioned doubts. Computer modeling predicted that the thermal lesion extends between 1.64 and 1.85 mm around the MPD, which was relatively similar to the thickness of the whitish halo macroscopically observed immediately after the thermal ablation (~1 mm in Figure 8(A)) and very close to the extension of the coagulation necrosis seen in the

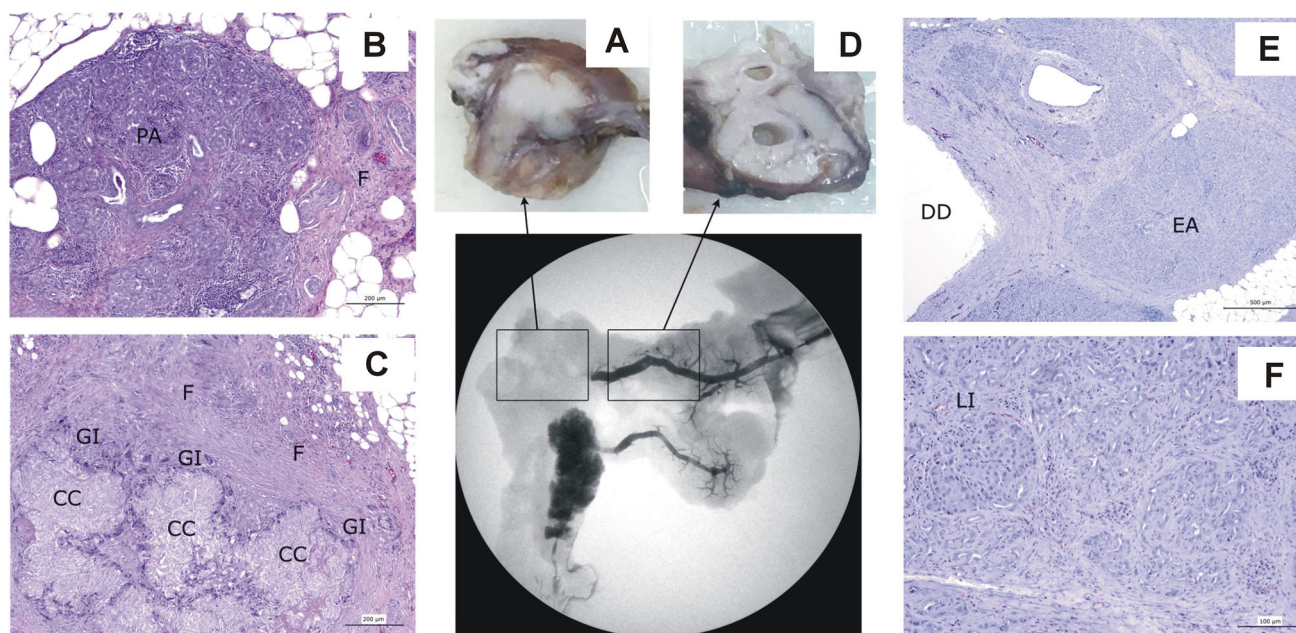


Figure 10. Animal model results. Histopathological findings of Group 30-day, distinguishing the ablation zone (A–C) and the distal zone (D–F). (A) Macroscopic view of the ablation zone. (B,C) Histological image (H&E). (B) Residual pancreatic tissue (PA) tissue with intense fibrosis (F). (C) Granulomas with cholesterol crystals (CC) surrounded by a granulomatous infiltrate (GI), with macrophages and giant cells and intense fibrosis (F). (D) Macroscopic view of distal portion in the main pancreas showing ducts dilation. (E,F) Histological image (H&E). (E) Ducts dilatation (DD) and complete and homogeneous exocrine atrophy (EA). (F) Langerhans islets (LI) preservation.

microscopic image in the animal study (~1.5 mm in Figure 8(C)). Furthermore, the fluoroscopy image in the animal setting revealed that the duct was patent, and even had areas of leakage, which may account for the risk of POPF in the clinical setting in the firsts two weeks PO in spite of MPD ablation.

After seven days PO, the ablated area in the animal study showed a cavity (0.5–1 cm diameter) with immature collagen tissue in the margins and partially atrophic pancreatic tissue. This matched well with the clinical results, which showed an MPD ablation area of 0.86 ± 0.29 cm. Interestingly, fluoroscopy images revealed two possible scenarios: effective closure of the duct in some animals, or an intrapancreatic dilatation along the ablation zone (with high levels of amylase fluid content in others, which might have digested the necrotic tissue, see Table 2), which again might account for the risk of POPF in the clinical setting in spite of duct ablation. After 30 days PO, the fluoroscopy images in the animal study revealed complete MPD occlusion. Interlobular fibrosis of the duct wall was found along the necrotic zone, along with complete homogeneous exocrine atrophy. Again, this finding matched well with CT images on patients over 30 days (see Figure 4), in which reduction of the pancreas diameter and the MPD were similar to those in the animals. The complete exocrine atrophy at 30-day PO also matched well with the complete exocrine insufficiency in patients at this stage, according to the need for pancreatic supplements in 87.5% of the patients.

Putting these data into perspective, we must acknowledge that the thickness of the pancreas measured by CT after PD has previously been used as a surrogate variable of pancreas atrophy and exocrine insufficiency. After PD, the gold standard is to reconstruct pancreas drainage by making

an anastomosis into the stomach or the small bowel. However, with this conventional reconstruction the incidence of pancreas insufficiency is high in the long term (usually over 50% [30–32]) and the reduction of pancreas thickness is also systematic (about 0.4 mm per month [22]), following a linear tendency that may not be very different to TAMPD in the long term.

Several limitations should also be addressed: First, clinical experience is still very limited (as corresponds to an IDEAL 2a stage study) to draw definitive conclusions. Second, the animal model and a clinical setting are relatively similar, but not identical for two reasons: (1) the pancreatic anatomy between animal and human is different and (2) in the animal model no pancreas anastomosis (as it was done in clinical setting) was performed to be able to study the real consequences of POPF after a simple TAMPD. And third, different RF ablation devices were used in the previous and current TAMPD pre-clinical studies. While we had previously used a bipolar RF catheter [12,13], the device used in the current context (ClosureFast[®] applicator) does not really apply RF current to the tissue, but the ablation zone is created by thermal conduction from the applicator surface, which reaches 80 °C. From our experience, we think that this method is inherently safer, since the maximum temperature in the tissue never exceeds this limit and the coating also avoids the tissue sticking.

5. Conclusions

TAMPD leads to long-term exocrine pancreatic atrophy because of complete occlusion of the MPD, usually beyond 30 days. Before 30 days, the occlusion might not be complete

and the created ablation zone may be short-lived and insufficient to avoid POPF due to ductal dilatation, possibly caused by digestion of the ablated (necrotic) area by the pancreatic juice during the two weeks after ablation.

Disclosure statement

No potential conflict of interest was reported by the author(s).

Funding

Spanish Ministerio de Ciencia, Innovación y Universidades/Agencia Estatal de Investigación (MCIN/AEI/10.13039/501100011033) under grants RTI2018-094357-B-C21 and RTI2018-094357-B-C22.

ORCID

Xavier Moll  <http://orcid.org/0000-0002-2992-9361>
 Dolors Fondevila  <http://orcid.org/0000-0001-7443-0175>
 Félix García-Arnas  <http://orcid.org/0000-0001-6651-3173>
 Juan J. Pérez  <http://orcid.org/0000-0001-8486-8699>
 Benedetto Ielpo  <http://orcid.org/0000-0003-3129-3208>
 Patricia Sánchez-Velázquez  <http://orcid.org/0000-0002-7902-3920>
 Luis Grande  <http://orcid.org/0000-0001-9146-9004>
 Enrique Berjano  <http://orcid.org/0000-0002-3247-2665>
 Fernando Burdio  <http://orcid.org/0000-0003-3038-0086>
 Anna Andaluz  <http://orcid.org/0000-0001-8097-8110>

Data availability statement

The data underlying this article will be shared on reasonable request to the corresponding author.

References

- [1] Howard JM, Hess W. History of the pancreas: mysteries of a hidden organ. Berlin/Heidelberg (Germany): Springer Science & Business Media; 2012.
- [2] Rösch W, Phillip J, Gebhardt C. Endoscopic duct obstruction in chronic pancreatitis. *Endoscopy*. 1979;11(1):43–46.
- [3] Schneider MU, Meister R, Domschke S, et al. Whipple's procedure plus intraoperative pancreatic duct occlusion for severe chronic pancreatitis: clinical, exocrine, and endocrine consequences during a 3-year follow-up. *Pancreas*. 1987;2(6):715–726.
- [4] Tran K, Van Eijck C, Di Carlo V, et al. Occlusion of the pancreatic duct versus pancreaticojejunostomy: a prospective randomized trial. *Ann Surg*. 2002;236(4):422–428; discussion 428.
- [5] Theodosopoulos T, Dellaportas D, Yiallourou AI, et al. Pancreatic remnant occlusion after Whipple's procedure: an alternative oncologically safe method. *ISRN Surg*. 2013;2013:960424.
- [6] Alfieri S, Agnes A, Rosa F, et al. Long-term pancreatic exocrine and endometabolic functionality after pancreaticoduodenectomy. Comparison between pancreaticojejunostomy and pancreatic duct occlusion with fibrin glue. *Eur Rev Med Pharmacol Sci*. 2018;22(13):4310–4318.
- [7] Alfieri S, Quero G, Rosa F, et al. Indications and results of pancreatic stump duct occlusion after duodenopancreatectomy. *Updates Surg*. 2016;68(3):287–293.
- [8] Mazzaferro V, Virdis M, Sposito C, et al. Permanent pancreatic duct occlusion with neoprene-based glue injection after pancreaticoduodenectomy at high risk of pancreatic fistula: a prospective clinical study. *Ann Surg*. 2019;270(5):791–798.
- [9] Reissman P, Perry Y, Cuenca A, et al. Pancreaticojejunostomy versus controlled pancreaticocutaneous fistula in pancreaticoduodenectomy for periampullary carcinoma. *Am J Surg*. 1995;169(6):585–588.
- [10] Fromm D, Schwarz K. Ligation of the pancreatic duct during difficult operative circumstances. *J Am Coll Surg*. 2003;197(6):943–948.
- [11] Goldsmith HS. Pancreatic duct ligation: an idea revisited. *J Am Coll Surg*. 2013;217(3):560–562.
- [12] Andaluz A, Ewertowska E, Moll X, et al. Endoluminal radiofrequency ablation of the main pancreatic duct is a secure and effective method to produce pancreatic atrophy and to achieve stump closure. *Sci Rep*. 2019;9(1):5928.
- [13] Ewertowska E, Andaluz A, Moll X, et al. Development of a catheter-based technique for endoluminal radiofrequency sealing of pancreatic duct. *Int J Hyperthermia*. 2019;36(1):677–686.
- [14] Ielpo B, Pueyo-Pérez EM, Radosevic A, et al. Clinical case report: endoluminal thermal ablation of main pancreatic duct for patients at high risk of postoperative pancreatic fistula after pancreaticoduodenectomy. *Int J Hyperthermia*. 2021;38(1):755–759.
- [15] Marcus HJ, Bennett A, Chari A, et al. IDEAL-D framework for device innovation: a consensus statement on the preclinical stage. *Ann Surg*. 2022;275(1):73–79.
- [16] Almeida JI, Kaufman J, Göckeritz O, et al. Radiofrequency endovenous closure FAST versus laser ablation for the treatment of great saphenous reflux: a multicenter, single-blinded, randomized study (RECOVERY study). *J Vasc Interv Radiol*. 2009;20(6):752–759.
- [17] Thompson RB, Esch BD, Dhaka VK, et al. Methods for treatment a hollow anatomic structure. United States patent US 7,828,793 B2. 2010 Nov 9.
- [18] Investigational device exemptions (IDEs) for early feasibility medical device clinical studies, including certain first in human (FIH) studies. Guidance for industry and food and drug administration staff. U.S. Department of Health and Human Services. Rockville (MD): Food and Drug Administration. Center for Devices and Radiological Health. Center for Biologics Evaluation and Research; 2013. Available from: www.fda.gov/media/81784/download
- [19] Callery MP, Pratt WB, Kent TS, et al. A prospectively validated clinical risk score accurately predicts pancreatic fistula after pancreaticoduodenectomy. *J Am Coll Surg*. 2013;216(1):1–14.
- [20] Dindo D, Demartines N, Clavien PA. Classification of surgical complications: a new proposal with evaluation in a cohort of 6336 patients and results of a survey. *Ann Surg*. 2004;240(2):205–213.
- [21] Bassi C, Marchegiani G, Dervenis C, et al. The 2016 update of the international study group (ISGPS) definition and grading of postoperative pancreatic fistula: 11 years after. *Surgery*. 2017;161(3):584–591.
- [22] Quesada R, Simón C, Radosevic A, et al. Morphological changes of the pancreas after pancreaticoduodenectomy. *Sci Rep*. 2019;9(1):14517.
- [23] Hsagall PA, Di Gennaro F, Baumgartner C, et al. IT'IS database for thermal and electromagnetic parameters of biological tissues. Version 4.1. 2022. Available from: itis.swiss/database
- [24] Pérez JJ, Berjano E, González-Suárez A. In-silico modeling to compare radiofrequency-induced thermal lesions created on myocardium and thigh muscle. *Bioengineering*. 2022;9(7):329.
- [25] Mitchell HH, Hamilton TS, Steggerda FR, et al. The chemical composition of the adult human body and its bearing on the biochemistry of growth. *J Biol Chem*. 1945;158(3):625–637.
- [26] McCulloch P, Altman DG, Campbell WB, et al. No surgical innovation without evaluation: the IDEAL recommendations. *Lancet*. 2009;374(9695):1105–1112.
- [27] Nentwich MF, El Gammal AT, Lemcke T, et al. Salvage completion pancreatectomies as damage control for post-pancreatic surgery complications: a single-center retrospective analysis. *World J Surg*. 2015;39(6):1550–1556.

- [28] Radosevic A, Quesada R, Serlavos C, et al. Microwave versus radiofrequency ablation for the treatment of liver malignancies: a randomized controlled phase 2 trial. *Sci Rep.* 2022;12(1):316.
- [29] Quesada R, Moreno A, Poves I, et al. The impact of radiofrequency-assisted transection on local hepatic recurrence after resection of colorectal liver metastases. *Surg Oncol.* 2017;26(3):229–235.
- [30] Sabater L, Calvete J, Aparisi L, et al. Neoplasias de páncreas y periampulares: morbimortalidad, resultados funcionales y supervivencia a largo plazo [pancreatic and periampullary tumors: morbidity, mortality, functional results and long-term survival]. *Cir Esp.* 2009;86(3):159–166. Spanish.
- [31] Fang WL, Su CH, Shyr YM, et al. Functional and morphological changes in pancreatic remnant after pancreaticoduodenectomy. *Pancreas.* 2007;35(4):361–365.
- [32] Tomimaru Y, Takeda Y, Kobayashi S, et al. Comparison of postoperative morphological changes in remnant pancreas between pancreaticojejunostomy and pancreaticogastrostomy after pancreaticoduodenectomy. *Pancreas.* 2009;38(2):203–207.